Complete surface plasmon-polariton band gap and gap-governed waveguiding, bending and splitting

2009 J. Phys.: Condens. Matter 21 185010

(http://iopscience.iop.org/0953-8984/21/18/185010)

IOP Publishing Journal of Physics: Condensed Matter

J. Phys.: Condens. Matter **21** (2009) 185010 (6pp) doi:10.1088/0953-8984/21/18/185010

Complete surface plasmon-polariton band gap and gap-governed waveguiding, bending and splitting

Fengqin Wu[1], **Dezhuan Han**[2], **Xinhua Hu**[3], **Xiaohan Liu**[1,3] **and Jian Zi**[1,3]

[1] Surface Physics Laboratory and Department of Physics, Fudan University, Shanghai 200433, People's Republic of China
[2] Department of Physics, The Hong Kong University of Science and Technology, Clear Water Bay, Kowloon, Hong Kong, People's Republic of China
[3] Laboratory of Advanced Materials, Fudan University, Shanghai 200433, People's Republic of China

E-mail: huxh@fudan.edu.cn and jzi@fudan.edu.cn

Received 29 December 2008, in final form 27 February 2009
Published 24 March 2009
Online at stacks.iop.org/JPhysCM/21/185010

Abstract

We show theoretically that a complete band gap for surface plasmon-polaritons (SPPs) can exist in a flat metal surface coated with a two-dimensional periodic array of dielectric cylinders. Based on the SPP band gap, gap-governed SPP waveguides, bends and splitters at telecom wavelengths can be achieved by introducing line defects. Numerical simulations show that the proposed SPP waveguides have a very low loss, while SPP bends and splitters can bend and split guided SPPs efficiently. The proposed SPP waveguides, bends and splitters could thus be exploited to construct compact integrated optical circuits in the emerging field of plasmonics.

(Some figures in this article are in colour only in the electronic version)

1. Introduction

In recent years surface plasmon-polaritons (SPPs) have attracted considerable attention due to their potential applications in the emerging field of plasmonics. SPPs are collective electron density oscillations bound at metal–dielectric interfaces and can propagate in a wave-like fashion along the interfaces [1]. Owing to their subwavelength and low-dimensional nature, SPPs can be exploited to transport light energy beyond the diffraction limit of conventional dielectric optics, leading to compact integrated optical circuits [2–4]. To achieve such a goal, much effort has been made to introduce different kinds of SPP waveguides such as metal V-grooves [5], metal stripes [6], metal nanoparticle chains [7] and dielectric stripes on a metal surface [8].

It is known that the propagation of electromagnetic waves is absolutely forbidden for frequencies within the complete band gaps of photonic crystals [9–11]. Based on complete photonic band gaps, channel waveguides and bends can be obtained by introducing line defects [12, 13]. The waveguiding is governed by photonic band gaps, fundamentally different from conventional dielectric waveguides. As in photonic crystals, SPPs will experience multiple Bragg scatterings when propagating along periodic metallic structures, leading to complicated band structures and band gaps [14–17]. By introducing line defects in periodic arrays of metal bumps placed on a metal surface, gap-governed SPP waveguiding and bending has been observed [18, 19]. The waveguiding and bending efficiencies are, however, rather low due to the strong scattering loss at boundaries and the intrinsic loss of the metal surface and bumps. SPP waveguides and bends with low loss and high efficiency are very desirable.

It has been shown [16, 20–23] that a flat metal surface or a film coated with a periodically textured dielectric layer displays well-defined SPP band structures, and SPPs can be directly excited externally from free space. No complete band gaps, however, have been reported in such systems. In this paper we show theoretically that complete SPP band gaps can be obtained in a flat metal surface coated with a two-dimensional periodic array of dielectric cylinders as long as the structural and optical parameters of the dielectric coating layer are properly chosen. Based on complete SPP band gaps,

gap-governed SPP waveguides, bends and splitters at telecom wavelengths are proposed.

2. Results and discussions

The proposed SPP waveguides, bends and splitters rely on a structure consisting of a metal surface coated with a two-dimensional periodic array of dielectric cylinders. Dielectric cylinders have a square cross-section and are arranged in a square lattice. The two-dimensional periodic array of dielectric cylinders has the following structural parameters: lattice constant a, cylinder side width b and cylinder height t. The lattice constant and cylinder side width are taken to be $a = 640$ nm and $b = 320$ nm, while the cylinder height is taken to be $t = 2$ μm in the following designs for SPP straight waveguides, bends and splitters. The choice of these values renders a working wavelength at telecom wavelengths for the proposed SPP waveguides, bends and splitters.

Without loss of generality, the metal is chosen to be Au, the refractive index of which is taken from [24]. The dielectric cylinders are assumed to be made of Si_3N_4 (with a refractive index of 2.0 at telecom wavelengths). The choice of Si_3N_4 lies in the following factors. First, Si_3N_4 is nearly lossless at telecom wavelengths such that it has been widely used in the fabrications of optical waveguides. Second, Si_3N_4 fabrication and patterning are mature and fully compatible with micromanufacturing technologies. Thus our proposed structures are feasible from the fabrication point of view. Third, the refractive index of Si_3N_4 is relatively large for opening up a complete SPP band gap, as will be shown later. No complete SPP band gap exists if a dielectric material with a low refractive index is chosen [22].

A finite-difference time-domain (FDTD) method [25] is used in numerical simulations. Within the framework of this method, it is possible to calculate band structures and field distributions. Periodic or perfectly matched layer (PML) boundary conditions [26] are adopted depending on the systems dealt with. In the present work, we only consider TM polarized modes (with the magnetic field parallel to the metal surface). The grid sizes in our calculations are 40 nm × 40 nm × 40 nm in the three directions.

2.1. Band structure and complete SPP band gap

To calculate the optical response of a metal surface coated with a two-dimensional periodic array of dielectric cylinders, a number of random TM polarized electric sources are placed in the computational domain at time $t = 0$. The time monitors at random points record time evolution of the electric fields. Their Fourier transformations can give power spectra [27] from which we can obtain the band structures of the modes supported by the structure. For band structure calculations, periodic boundary conditions are used in the in-plane, and PML boundary conditions are applied in the direction normal to the metal surface.

Figure 1 shows the calculated band structures of the modes supported for different cylinder heights. The structure under study supports two kinds of surface waves: one is SPPs that are bound at the metal–dielectric interface and the other is guided modes with fields confined to the dielectric layer, revealed by inspecting the field distributions. Guided modes are sensitive to the cylinder height as expected. For small cylinder heights, guided modes lie in high frequencies which are outside the displayed frequency range in figure 1(a). For a cylinder height comparable to the telecom wavelengths, guided modes may coexist with SPP modes (figure 1(b)). In figures 1(a) and (b) the PML absorbing layer is separated from the top of the dielectric cylinders by a distance of about 3 μm. For large cylinder heights more guided modes appear. Moreover, SPP modes are kept unchanged regardless of the cylinder height. For very large cylinder heights the PML absorbing layer is just attached to the top of the dielectric cylinders. As a result, guided modes are absorbed by the PML absorbing layer.

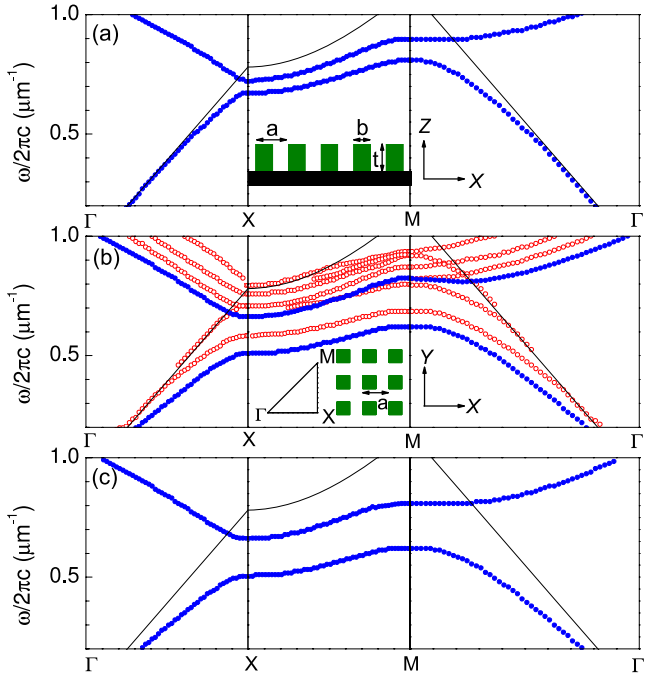

Figure 1. Calculated band structures for a Au surface coated with a periodic array of Si_3N_4 cylinders arranged in a square lattice. The cylinder height is (a) 0.2 μm, (b) 2 μm and (c) semi-infinite. Side and top views of the structure under study are shown in the insets of (a) and (b), respectively. Γ, X and M are points of high symmetry in the first Brillouin zone. Solid (open) circles denote SPP (guided) modes. Solid lines represent the light line of air.

For the semi-infinite cylinder height a complete SPP band gap exists between the first and second SPP bands with wavelength ranging from 1.51 to 1.61 μm, as shown in figure 1(c). The ratio of the band gap width to the mid-gap frequency is about 6.4%. The lower gap edge is determined by the M point while the upper gap edge is determined by the X point. The existence of a complete SPP band gap is due to strong multiple Bragg scatterings when propagating along the Au surface, similar to photonic band gaps in photonic crystals [9–11]. For a cylinder height much larger than corresponding gap wavelengths, the position and width of the SPP band gap are almost identical to those for the semi-infinite

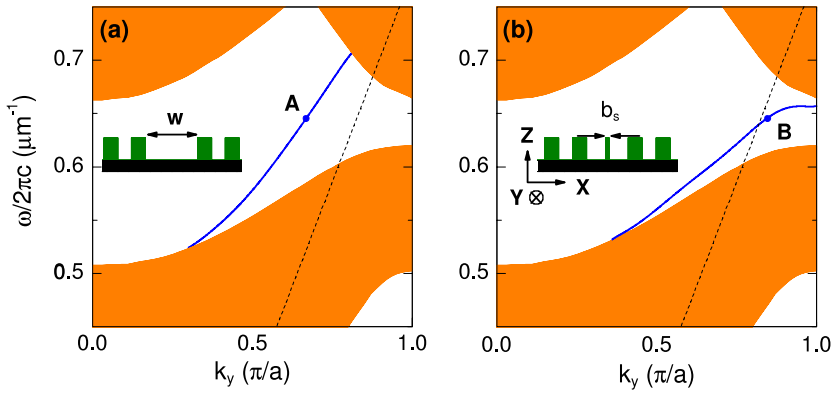

Figure 2. Projected SPP band structures for two designs of SPP waveguides. (a) Changing the distance between two adjacent rows of cylinders from a to $b + w$ with $w = 1.2$ μm. (b) Replacing a row of cylinders with a Si_3N_4 strip of width $b_s = 80$ nm. The side view of the corresponding structures is shown in the insets. Colored (white) regions denote the projected SPP bands (band gaps). Solid and dashed lines represent SPP defect modes and the light line of air, respectively. Modes A and B are at wavelength of 1.55 μm.

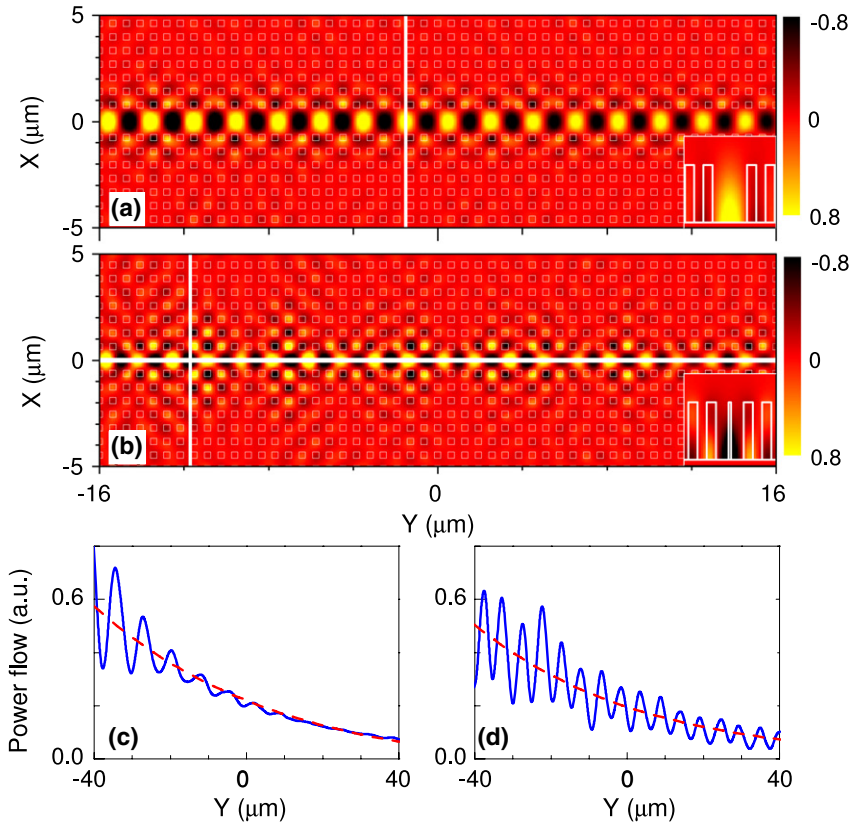

Figure 3. (a) Distributions of the z-component of electric fields in the plane above the Au surface by a distance of 20 nm for mode A of figure 2(a). The inset is the transverse cross-section profile of the z-component of electric fields at the white line in (a). (b) The same as in (a) but for mode B of figure 2(b). The dielectric cylinders are outlined by white lines. (c), (d) Power flows (solid lines) along the line $x = 0$ for (a) and (b), respectively. Dashed lines are fitted curves by an exponential function.

cylinder height (figure 1(b)). With the decrease in the cylinder height, the width of SPP band gap decreases. For a cylinder height much smaller than gap wavelengths, no complete SPP band gaps exist (figure 1(a)). This can be understood by the fact that the decay length of SPPs on the dielectric layer side is much larger than the cylinder height. As a result, multiple Bragg scatterings are not strong enough to open up a complete SPP band gap.

2.2. SPP straight waveguide

The existence of a complete SPP band gap has important consequences. The propagation of SPPs is absolutely forbidden for frequencies within the complete SPP band gap. Like in photonic crystals [12], SPPs can be guided by introducing line defects. We first consider a SPP waveguide by enlarging the distance between two adjacent rows of dielectric

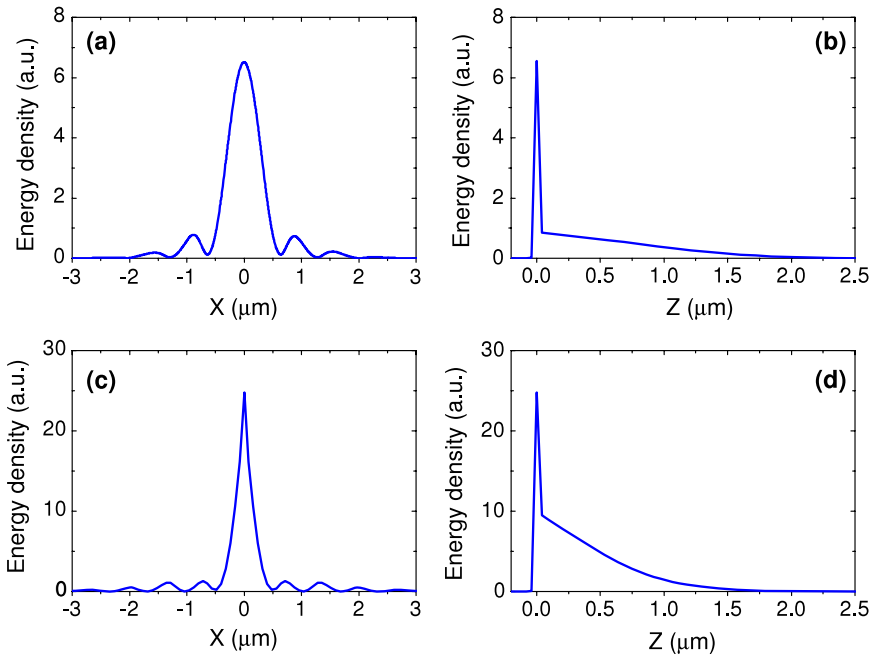

Figure 4. (a) Electromagnetic energy density profile along the x direction for mode A at the Au surface. (b) Electromagnetic energy density profile along the z direction for mode A at the middle of the waveguide. (c), (d) The same as (a) and (b) but for mode B.

cylinders from a to $b + w$ (where $w > a - b$ is the waveguide width). Figure 2(a) shows the projected SPP band structures for the waveguide with $w = 1.2$ μm and $t = 2.0$ μm. A single SPP waveguide mode appears in the SPP band gap. With increasing w this mode shifts towards, but remains above, the light line of air. As a result, this SPP waveguide mode will suffer a radiation loss due to its coupling into propagating modes in air.

To suppress the radiation loss one can lower the SPP waveguide mode below the light line of air. This can be achieved by replacing a row of cylinders by a dielectric stripe of width b_s and the same height. Figure 2(b) shows the projected SPP band structures with $b_s = 80$ nm and $t = 2.0$ μm. The SPP waveguide mode at the telecom wavelength of 1.55 μm is now below the light line of air. The introduction of the dielectric stripe will alter the dispersion of the SPP guided mode. With increasing b_s the SPP guided mode shifts systematically towards and eventually merge into the lower SPP band. In the meantime new SPP guided modes appear. Multiple SPP guided modes occur in the gap frequency region if the stripe width is larger than 320 nm.

Basically, there are two channels for propagation losses: the radiation loss from the coupling into propagating modes in air and absorption by the structure. To obtain the propagation length, we carry out simulations of above two waveguides with a finite length of 100 μm. SPP waveguide modes are excited by a TM polarized Gaussian beam with a wavelength of 1.55 μm and a full width at half maximum (FWHM) of 400 nm at one end. PML boundary conditions are applied in three dimensions. Figure 3 shows the electric field distributions a distance of 20 nm above the Au surface. It can be seen that the electric fields are highly confined to the line defect regions and bound to the Au surface. Figures 3(c) and (d) show the power flow along the waveguide, defined as the y component of the Poynting vector. By fitting the power flow to an exponentially decaying curve, the propagation length can be derived, about $L_{SPP} = 42.2$ μm and 40.2 μm for the waveguide modes A and B, respectively. If the metal absorption is neglected, $L_{SPP} = 55.5$ μm and infinity can be found for modes A and B, respectively. This implies that the propagation loss comes mainly from the radiation loss for mode A and from the absorption loss of metal for mode B. The metal absorption is larger for mode B than for mode A since mode B has a much smaller group velocity.

To explore the lateral confinement of SPP guided modes, their electromagnetic energy density [28] is calculated, as shown in figure 4. Obviously, SPP guided modes are sharply confined in the line defect region and decay rapidly away from the metal–dielectric interface. With the electromagnetic energy density profiles we can obtain the mode area A_m [28] for SPP guided modes. The normalized mode area $A_n = A_m/(\lambda/2)^2$ is a fair measure of the energy confinement of the SPP waveguide modes. The normalized mode area for waveguide modes A and B is, respectively, 0.22 and 0.147 which are only small fractions of the diffraction-limited area in free space. Furthermore, with the absolute values of L_{SPP} and A_m we can also evaluate the figure of merit (FOM) for SPP guided modes, namely $M = 2L_{SPP}\sqrt{\pi/A_m}$ [29]. The resulting FOM for modes A and B is 412 and 480, respectively.

2.3. SPP 90° bend and splitter

Optical bends and splitters are essential elements for integrated photonic circuits. Conventional dielectric waveguides suffer a serious radiation loss if they are sharply bent with a radius smaller than the working wavelength. Due to the confinement

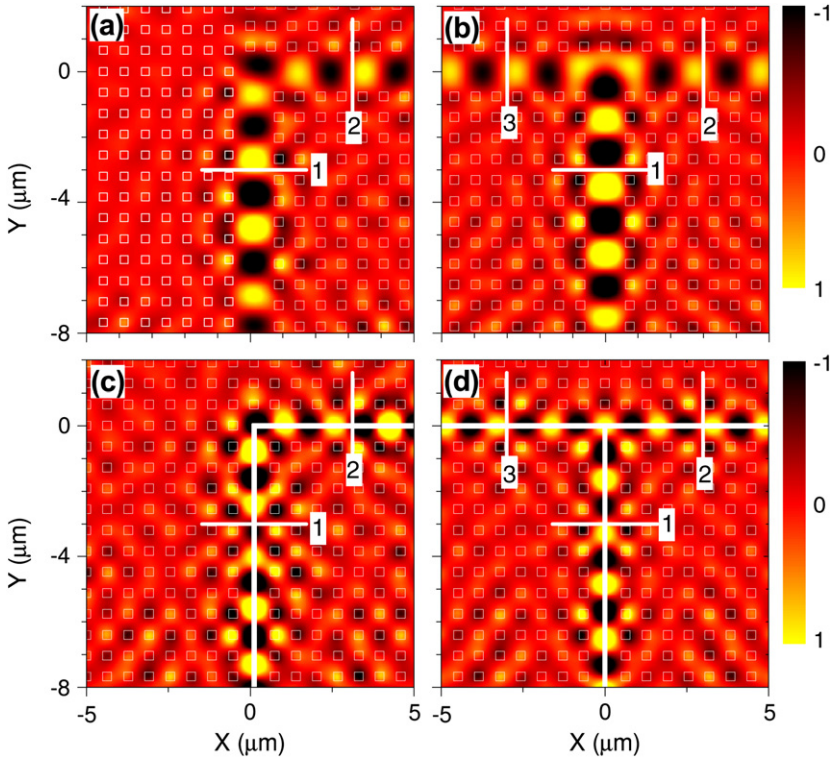

Figure 5. Distributions of the z-component of electric fields in the plane above the Au surface by a distance of 20 nm. (a) SPP 90° bend and (b) SPP splitter for mode A of figure 2(a). The widths of both horizontal and vertical waveguides are the same with $w = 1.2$ μm. (c), (d) The same as in (a) and (b) but for mode B of figure 2(b). The dielectric cylinders and stripes are outlined by white lines.

effects of photonic band gaps, sharp 90° bends with a high efficiency have been demonstrated [13]. Here, we show that highly efficient SPP 90° bends and splitters are also possible. Figure 5 shows the performance of SPP 90° bends and splitters based on the SPP waveguide modes A and B of figure 2. The bending efficiency is calculated by $T = I_2/I_1$, where I_1 (I_2) is the integrated incident (outgoing) power flow at the core region of the waveguides indicated by line 1 (line 2). The splitting efficiency is calculated by $S = (I_2 + I_3)/I_1$, where I_1, I_2 and I_3 are the integrated power flows at the core region of the waveguides indicated by lines 1, 2 and 3, respectively. A high bending efficiency of $T = 82.6\%$ and 75.3% is obtained for the SPP bends shown in figures 5(a) and (c), respectively. For SPP splitters shown in figures 5(b) and (d) a splitting efficiency of $S = 83.4\%$ and 78.4%, respectively, is found. Note that the bending and splitting efficiencies could be further improved by optimizations, which is beyond the scope of the present paper.

3. Conclusions

In summary, we studied theoretically the optical response of a flat Au surface coated with a two-dimensional periodic array of Si_3N_4 cylinders. Complete SPP band gaps were found in such a structure. By introducing line defects, SPP waveguides, bends and splitters working at telecom wavelengths were proposed. Numerical simulations showed that the proposed SPP waveguide has a large propagation length of more than 40 μm. The bending and splitting efficiencies of our proposed SPP bends and splitters are more than 80%. Our results indicate that flat metal surfaces coated with periodically textured dielectric layers represent a promising approach in the construction of integrated plasmonic circuits.

Acknowledgments

This work is supported by the 973 Program (grant nos. 2007CB613200 and 2006CB921700). The research of XHL and JZ is further supported by the NSFC and Shanghai Science and Technology Commission.

References

[1] Raether H 1998 *Surface Plasmons* (Berlin: Springer)
[2] Barnes W L, Dereux A and Ebbesen T W 2003 *Nature* **424** 824
[3] Zayats A V, Smolyaninov I I and Maradudin A A 2005 *Phys. Rep.* **408** 131
[4] Maier S A 2007 *Plasmonics: Fundamentals and Applications* (New York: Springer)
[5] Bozhevolnyi S I, Volkov V S, Devaux E, Laluet J-Y and Ebbesen T W 2006 *Nature* **440** 508
[6] Zia R, Schuller J A and Brongersma M L 2006 *Phys. Rev.* B **74** 165415
[7] Maier S A, Kik P G, Atwater H A, Meltzer S, Harel E, Koel B E and Requicha A A G 2003 *Nat. Mater.* **2** 229
[8] Karalis A, Lidorikis E, Ibanescu M, Joannopoulos J D and Soljačić M 2005 *Phys. Rev. Lett.* **95** 063901
[9] Yablonovitch E 1987 *Phys. Rev. Lett.* **58** 2059
[10] John S 1987 *Phys. Rev. Lett.* **58** 2486
[11] Joannopoulos J D, Meade R D and Winn J N 1995 *Photonic Crystals* (Princeton, NJ: Princeton University Press)

[12] Mekis A, Fan S and Joannopoulos J D 1998 *Phys. Rev.* B **58** 4809
[13] Mekis A, Chen J C, Kurland I, Fan S, Villeneuve P R and Joannopoulos J D 1996 *Phys. Rev. Lett.* **77** 3787
[14] Kitson S C, Barnes W L and Sambles J R 1996 *Phys. Rev. Lett.* **77** 2670
[15] Kretschmann M and Maradudin A A 2002 *Phys. Rev.* B **66** 245408
[16] Gérard D, Salomon L, de Fornel F and Zayats A V 2004 *Phys. Rev.* B **69** 113405
[17] Kelf T A, Sugawara Y, Baumberg J J, Abdelsalam M and Bartlett P N 2005 *Phys. Rev. Lett.* **95** 116802
[18] Bozhevolnyi S I, Erland Leosson J K, Skovgaard P M W and Hvam J M 2001 *Phys. Rev. Lett.* **86** 3008
[19] Marquart C, Bozhevolnyi S I and Leosson K 2005 *Opt. Express* **13** 3303
[20] Yoon J, Lee G, Song S H, Oh C-H and Kim P-S 2003 *J. Appl. Phys.* **94** 123
[21] Wedge S, Wasey J A E, Barnes W L and Sage I 2004 *Appl. Phys. Lett.* **85** 182
[22] Han D Z, Wu F Q, Li X, Xu C, Liu X H and Zi J 2006 *Appl. Phy. Lett.* **89** 091104
[23] Li X, Han D Z, Wu F Q, Xu C, Liu X H and Zi J 2008 *J. Phys.: Condens. Matter* **20** 485001
[24] Palik E D (ed) 1985 *Handbook of Optical Constants of Solids* vol 1 (New York: Academic) p 286
[25] Taflove A 1995 *Computational Electrodynamics: the Finite-Difference Time-Domain Method* (Boston, MA: Artech House)
[26] Berenger J P 1994 *J. Comput. Phys.* **114** 185
[27] Crozier K B, Lousse V, Kilic O, Kim S, Fan S and Solgaard O 2006 *Phys. Rev.* B **73** 115126
[28] Oulton R F, Sorger V J, Genov D A, Pile D F P and Zhang X 2008 *Nat. Photonics* **2** 496
[29] Buckley R and Berini P 2007 *Opt. Express* **15** 12174